

Performance of Local Ventilation System Combined with Underfloor Air Distribution as Preventative Measures for Infectious Diseases in Consulting Room

Jun Yoshihara¹, Toshio Yamanaka¹, Narae Choi², Tomohiro Kobayashi¹,
Noriaki Kobayashi¹, Aoi Fujiwara¹

*1 Osaka University
2-1 Yamadaoka
Suita City, Japan*

*2 Toyo University
5 Chome-28-20 Hakusan
Tokyo, Japan*

**Corresponding author:
yoshihara_jun@arch.eng.osaka-u.ac.jp*

ABSTRACT

This research introduces the local exhaust system (hood) into the consulting room to prevent airborne infection, especially for close-distance conversation. The hood's capture efficiency is mainly affected by surrounding air flow, so this research compared three various underfloor air distribution systems (UFAD); floor-supply displacements ventilation (FSDV), displacement-flow-type diffuser, and swirling flow type diffuser. FSDV is a displacement ventilation method where SA comes from the whole floor through carpets or panels, forming a tranquil up-flow. A displacement-flow-type diffuser forms thermal stratification by supplying horizontal flow along the floor. Swirling-type flow diffuser supplies up and swirling flow and mixes room air well. Droplet nuclei or microdroplets leaked from the hood should be exhausted without expanding to reduce infection risk. The lower hood capture efficiency is not directly relevant to the higher infection risk, and the route to the exhaust outlet could be significant. For this reason, FSDV is expected to reduce the infection risk for close-distance conversation compared to a swirling flow-type diffuser. Full-scale experiments were carried out in this research to reveal the relationship between the ventilation system (hood and three UFAD systems) and infection risk.

KEYWORDS

Local exhaust system, Floor-supply displacements ventilation, Wells-Riley model, Consulting room, Close-distance conversation

1 INTRODUCTION

Airborne infection caused by droplet nuclei and micro droplets moving as an aerosol is regarded as one of the possible ways to infect SARS-CoV-2 (World Health Organization, 2020). Though various measures have been taken to prevent it in many places, entire system-scale ventilation might not be enough to become the solution for preventing short-range airborne transmission (Federation of European Heating Ventilation and Air Conditioning Associations, 2020). Still, many scenarios cannot avoid close-distance conversations, for example, in a consulting (examination) room, restaurant, or crowded train. Therefore, this study proposes a novel approach combining a local exhaust ventilation system (LEV) and floor-supply displacement ventilation (FSDV)(Akimoto et al., 1997) in the consulting room. In FSDV, the conditioned air is supplied from the entire floor through many small halls or carpets, not through some diffusers. Because the capture performance of LEV is significantly affected by surrounding airflow (Komori et al., 2022), the FSDV system, which can make a calm airflow field (Akimoto et al., 1997), is expected to help LEV's performance. This report aimed to

evaluate the effectiveness of the combination of air conditioning with FSDV and a hood and its performance as an infection control measure.

2 METHOD AND MATERIALS

2.1 Measurement setting and case conditions.

A cross-sectional view of the experimental room is shown in Figure 1(a), and an isometric view is shown in Figure 1(b). The experimental room consists of $x=2,400$ $y=3,800$ $z=2,200$ mm and an under-floor chamber, where outside air cleaned by a HEPA filter is supplied under the floor and then blown into the room by a three-way floor outlet. The air supply rate is fixed at $1,000$ m^3/h (50 ACH). Exhaust air is exhausted at a total rate of 990 m^3/h through the local exhaust ventilation system (hood) shown in Figure 1(c) and general ceiling exhaust vents to balance the flow rate, and the room is designed as a clean room to maintain positive pressure. In addition, two human bodies simulating an infected person and a non-infected person (heating at 75 W/body) were placed in the room with an interval of $1,200$ mm in front of their mouths. A flanged hood is used because the flanged hood had the best capture performance under crosswind airflow in a previous study (Fig. 1(c))(Komori et al., 2022).

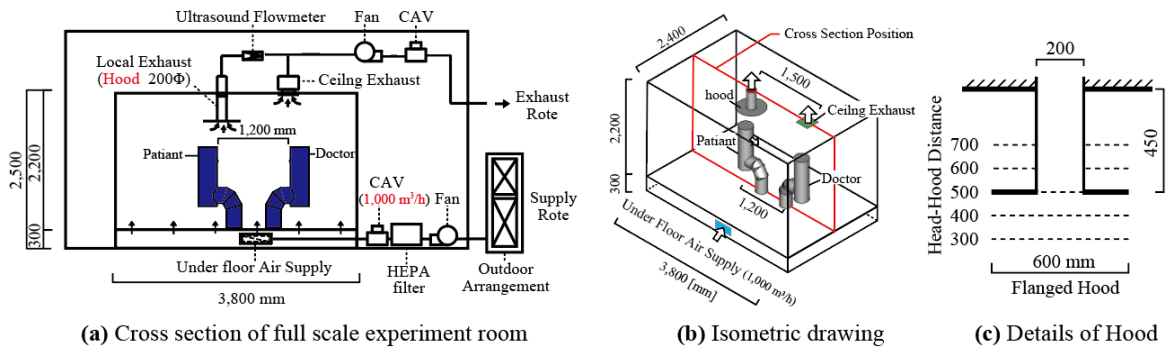


Fig.1 Full scale experiment setting

Table 1 shows the experimental conditions. The experiments were conducted assuming an examination room (Case A) and a non-examination room (Case B), and the hood exhaust volume was varied in eight ways for each of the three air supply methods. In Case A (examination room), a patient is assumed to be talking with a doctor in an infected state. In contrast, in Case B (non-examination room), since the location of the infected person cannot be specified, a hood is fixed between the human bodies, and a desk is set up as a realistic introduction position. Figure 3 shows the floor surfaces of the three air supply methods to be compared. The three air supply systems are floor-supply displacement ventilation (FSDV), swirling-flow type floor diffuser, and displacement ventilation type floor diffuser. In the FSDV system, the fresh outdoor air is supplied from the entire floor surface at a low air velocity (0.03 m/s) to form a calm airflow. In the swirling-flow type floor diffuser, the fresh outdoor air is supplied from eight swirling-flow floor diffusers with a swirl flow (air velocity: approx. $3\sim 4$ m/s) to form a well-mixed airflow. In the displacement ventilation type floor diffuser, the fresh outdoor air is supplied at an angle along the floor surface by 12 displacement ventilation type floor diffusers.

Table 1 Details of Experiment Parameter

	Air Supply Method from Under Floor Chamber	Air Flow Rate [m ³ /h] (Air Change Rate [1/h])	Hood Horizontal Position	Hood Flow Rate [m ³ /h]	Hood-Head Distance [mm]
Case A-1	Floor-supply ventilation	1,000 m ³ /h(50 /h)	above the infected person (patient)	0,50,100,150,200,300,400,500	500
Case A-2	8 Swirling flow type diffusers	1,000 m ³ /h (=125m ³ /h/diffuser×8) (50 /h)		0,50,100,150,200,300,400,500	500
Case A-3	12 Displacement flow type diffuser	1,000 m ³ /h (=83.3m ³ /h/diffuser×12) (50 /h)		0,50,100,150,200,300,400,500	500
Case B-1	Floor-supply ventilation	1,000 m ³ /h(50 /h)	middle of manikins	0,50,100,150,200,300,400,500	500
Case B-2	8 Swirling flow type diffusers	1,000 m ³ /h (=125m ³ /h/diffuser×8) (50 /h)		0,50,100,150,200,300,400,500	500
Case B-3	12 Displacement flow type diffuser	1,000 m ³ /h (=83.3m ³ /h/diffuser×12) (50 /h)		0,50,100,150,200,300,400,500	500

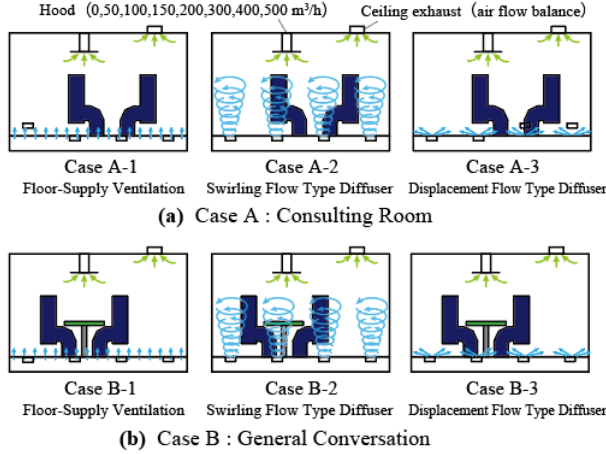


Fig.2 Concepts of Experimental Conditions

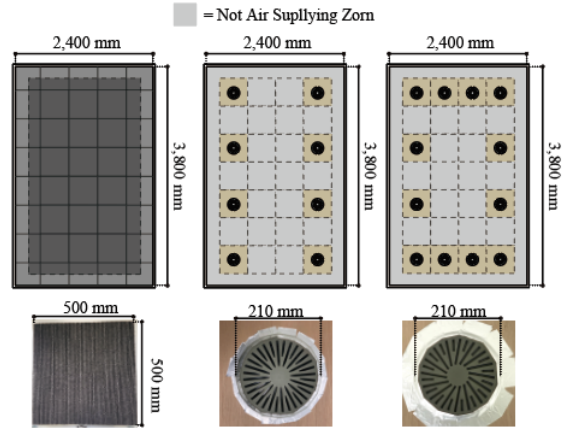


Fig.3 Floor details for each condition

2.2 Measurement point and Expiration condition

The exhaled breath of an infected person was reproduced by the simultaneous generation of CO₂ tracer gas and simulated saliva particles using a nebulizer. A conceptual diagram of exhalation generation is shown in Figure 4. CO₂ and helium were mixed at a ratio of 5:3 (CO₂: He = 3.26: 1.95 L/min) to equalize the density with that of air and generate at the height of the infected person's mouth (height: 1,100 mm) coupled with atomized simulated saliva. The expiratory volume, expiratory air velocity, and blow-off angle values during the conversation were obtained from a previous study(Zhang et al., 2022) and were set to 5.21 L/min, 0.30 m/s, and 11.9° vertical downward, respectively.

After the generation, the spatial distribution of the steady-state CO₂ concentration and the concentration in front of the mouth of non-infected subjects were measured. To account for the effects of evaporation and deposition, simulated saliva was atomized and sprayed simultaneously using a nebulizer (Figure 5). The viscosity of the simulated saliva was adjusted by adding 12 g of sodium chloride and 76 g of glycerin to 1 L of water, referring to previous research (Ogata et al., 2018). In order to reproduce the results obtained from the experiment of measuring expiratory air velocity and respiratory volume during the speech, as described in the previous report (Zhang et al., 2022), a 3D printer was used to create the air outlet (Figure 5 and Figure 7(d)).

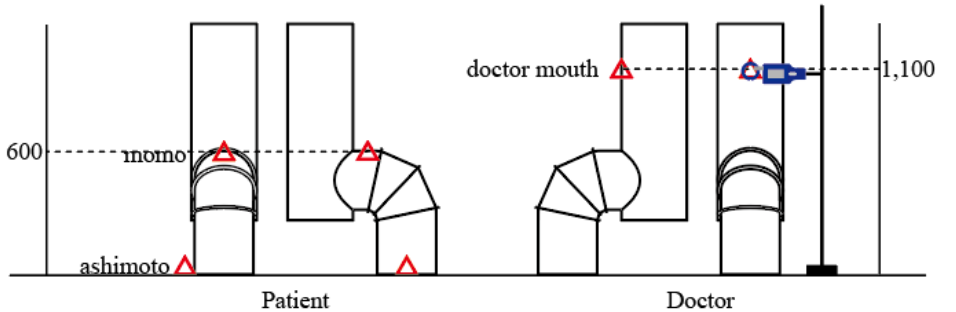
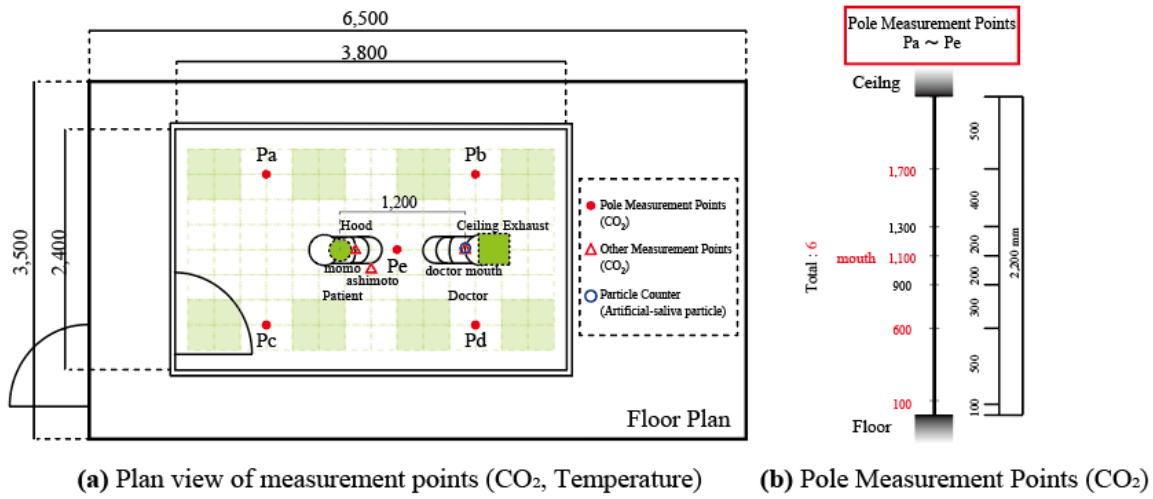
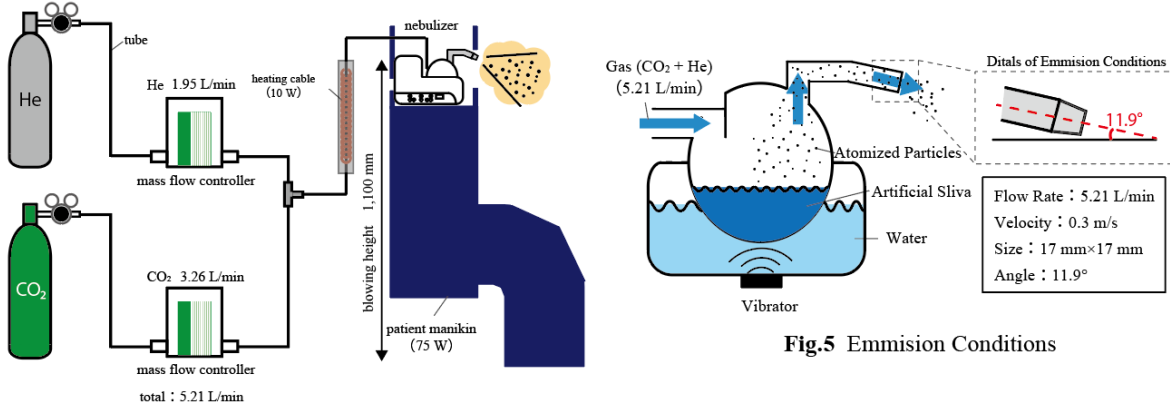


Fig.6 Measurement points (CO₂ gas concentration, Particle (> 0.3μm), Temperature)

2.3 Evaluation method

The hood capture efficiency: η , which indicates the percentage of the tracer gas generated that is collected by the hood, is calculated from Equation (1), and the effectiveness of the combination of the hood and air supply system is examined.

$$\eta = \frac{Q_h(C_h - C_{SA})}{Q_h(C_h - C_{SA}) + Q_e(C_e - C_{SA})} \quad (1)$$

where Q_h is hood flow rate [m³/h], C_h is tracer gas concentration of hood exhaust air [-], Q_e is ceiling exhaust flow rate [m³/h], C_e is tracer gas concentration of ceiling exhaust air [-], C_{SA} is tracer gas concentration of SA [-].

This study is based on the Wells&Riley model (Wells, 1955) (Riley EC et al., 1978) to evaluate infection control performance. The model defines one quanta as the unit of infectivity

that produces 63.2% of new infections in a closed space, and the basic equation is expressed in Equation (2).

$$P = 1 - e^{-n} \quad (2)$$

where P is an increased rate of the number of newly infected persons in closed space, n is the value of the quanta.

Based on the model, quanta concentration in front of the doctor's (non-infected person's) mouth; C_{qd} was calculated from equations (3). The quanta emission rate of 42 quanta/h calculated by REHVA(Federation of European Heating Ventilation and Air Conditioning Associations, 2020) was used as the quanta production rate for infected persons during the conversation.

$$C_{qd} = \frac{q}{Q} \cdot \frac{C_d}{C_{pm}} \quad (3)$$

where C_{dn} is the tracer gas concentration in front of the doctor's mouth normalized by perfect mixing concentration, C_d is the tracer gas concentration in front of the doctor's mouth, and C_{pm} is the tracer gas concentration at perfect mixing. Equation (3) can be calculated by changing C_d and C_p to CO_2 or simulated saliva particles.

Using the value of C_{qd} , the time until the infection risk of the doctor (non-infected person) reaches 5%; $t_{5\%}$ is calculated from Equation (4). Since the REHVA used the value of 5% when describing a sufficiently low risk of infection in an office. Therefore, this report uses 5% as a sufficiently low infection risk.

$$t(P\%) = -\frac{\ln(1 - P)}{n \cdot P} \quad (4)$$

2.4 Preliminary experiment on the nebulizer

To confirm the conversation reproducibility of the nebulizer, particle size and the number of particles were measured at the ceiling exhaust point (Figure 7(a)), immediately after the outbreak (Figure 7(b)), and in front of the doctor's mouth (Figure 7(c)). A hand-held particle counter (3889-01 KANOMAX) was used at the ceiling exhaust port and in front of the doctor's mouth, and a PDA (Dantec Fiber PDA) was used at the point immediately after the outbreak. D_s ; Sauter diameter was calculated using Equation (5) as representative particle size.

$$D_s = \frac{\sum n_i \cdot D_i^3}{\sum n_i \cdot D_i^2} \quad (5)$$

Where n_i is the number of pieces in each grain size category, and D_i is the representative diameter of each grain size category.

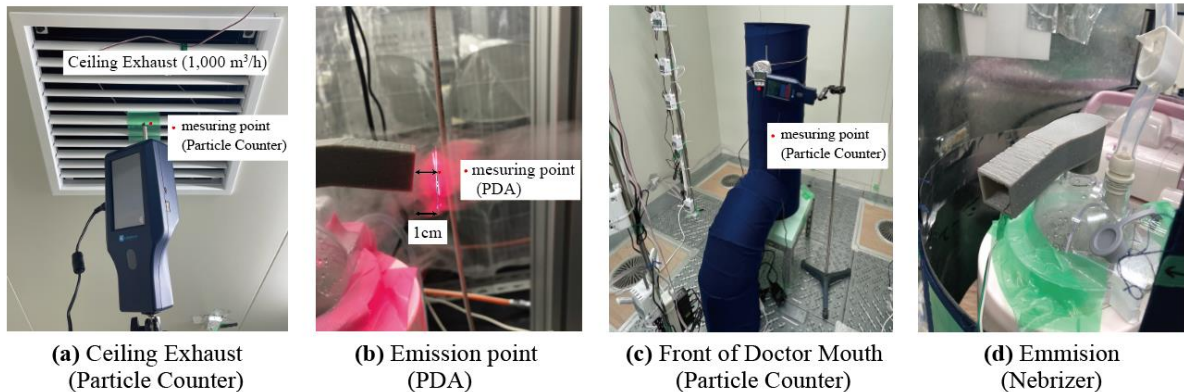


Fig.7 Picture of particle mesument

Figures 10(a), (b), and (d) show the particle size distribution and Sauter diameter calculated from the measurement results. Figure 10(c) shows the particle size distribution when counting the numbers in a previous study (Morawska et al., 2009). In the previous study, the particle size was $0.8\mu\text{m}$, while in the nebulizer used in this report, many large particles ($10\mu\text{m}$ or larger) with a strong tendency to settle out were generated. As a confirmation of steady-state conditions and a measurement of the background noise of particles, the time response variation of the number concentration measured at the exhaust point (generated over 70 minutes) is shown in Figure 8. Figure 8 shows that the background noise is low enough before and after the particle generation because air is supplied through a HEPA filter. Therefore, the particle concentration in front of the doctor's mouth was calculated, assuming the background particles were zero. In addition, even though the nominal ventilation time was only 1.2 minutes, the number concentration kept changing, suggesting that the nebulizer was not generating particles on a steady basis. After confirming that the background particle concentration was sufficiently small, the experiment was conducted with a steady-state waiting period of 5 minutes and a steady-state period of 15 minutes, as shown in Figure 9.

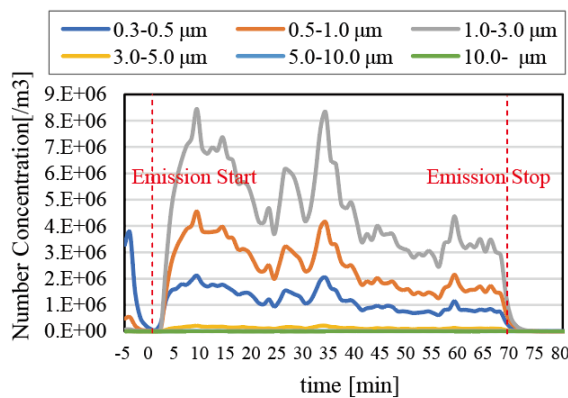


Fig.8 Number Concentration at Ceiling Exhaust

(Hood $0\text{ m}^3/\text{h}$, Ceiling Exhaust $1,000\text{ m}^3/\text{h}$, Swirling Typr Diffuser)

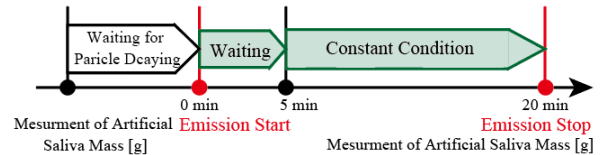


Fig.9 Experiment Time Schedule

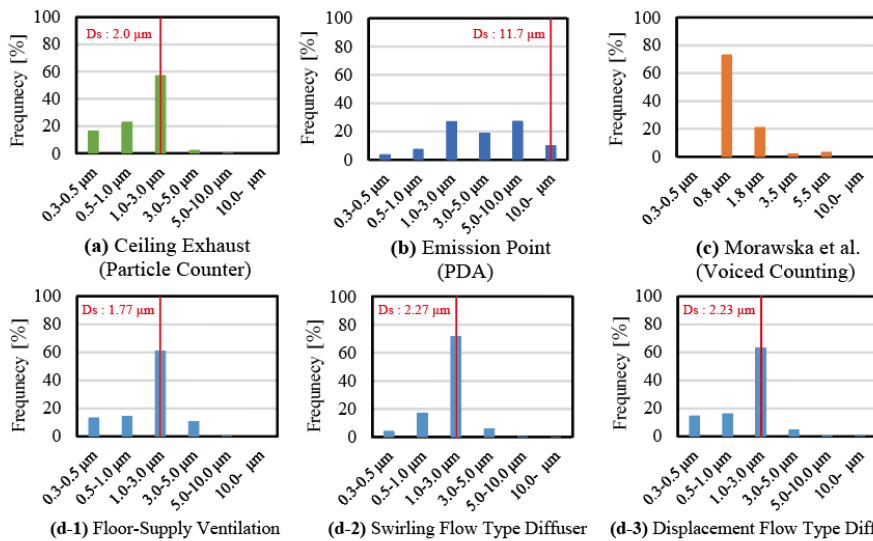


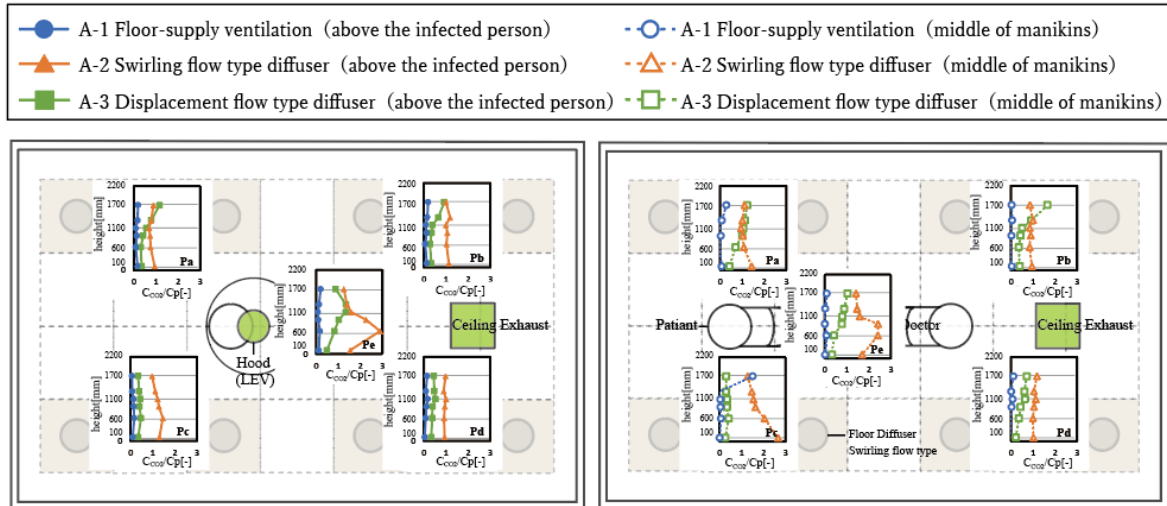
Fig.10 Frequency Distribution of Diffrent Mesurment Point (Comparson to Morawska et al.)

3 RESULTS AND DISCUSSION

3.1 The result calculated from CO_2 concentration

Figure 11 shows the spatial distribution of CO_2 tracer gas concentration normalized by the flow-

weighted concentration at the exhaust port under a hood exhaust volume of 100 m³/h (ceiling exhaust volume of 890 m³/h). In the case of FSDV, the normalized concentration is close to zero at all measurement points in both Case A (examination room) and Case B (non-examination room), indicating that exhaled air is exhausted in one direction immediately after its generation. In the displacement ventilation type floor diffuser, a concentration boundary surface was observed at some measurement points, suggesting the formation of an updraft. In the swirling-flow type floor diffuser, the existence of downward airflow is suggested near the exhalation point (Case A: Pe, Case B: Pa, Pc, Pe). At other measurement points, the normalized concentration is close to 1, and the exhaled air is mixed after descending. In the swirling flow type, the large blowing air velocity (about 3-4 m/s) is thought to cause a downward airflow due to the circulating flow between diffusers.



(a) Case A, Consulting room (Hood flow rate: 100 m³/h) (b) Case B, Restaurant, meeting room (Hood flow rate: 100 m³/h)

Fig.11 Normalized CO₂ concentration distribution

(C_{co2} = CO₂ concentration of each point, C_p = CO₂ concentration assuming perfect mixing)

Figure 12 shows the calculation results of hood capture efficiency and infection risk in Case A and Case B, calculated from CO₂ tracer gas using Equation (3). This indicates that the capture performance of the hood is greatly affected by the surrounding airflow. Therefore, the effectiveness of combining a hood and FSDV, which forms a quiet airflow, was confirmed. From Figure 12(c), when the infection risk is compared for each air supply method, the infection risk is lowest for the FSDV, and the value of $t_{5\%}$ consistently exceeds 24 hours, which is safe enough against infection. In the displacement ventilation type, when a hood is introduced (hood exhaust volume of 200 m³/h or more), the $t_{5\%}$ value exceeds 8 hours, assumed to be the maximum value of working hours, and can be considered relatively safe. On the other hand, for the swirling-flow type floor diffuser, the value of $t_{5\%}$ does not always exceed 8 hours and cannot be said to be safe.

Focusing on the results of Case B (outside the examination room) (Figure 12(a)) and comparing the results of Case A and Case B, the influence of the hood position was significant for the full-floor ventilation and displacement ventilation types, which form an upward airflow, and it is considered necessary to introduce a hood at a position where the exhaled air rises. Comparing the risk of infection for each air supply method (Figure 12(c)), the risk of infection is lowest for the FSDV, and the value of $t_{5\%}$ consistently exceeds 24 hours, which is safe enough against infection. In Case A, the infection risk decreases with the introduction of hoods in the FSDV and displacement ventilation type floor diffuser. In contrast, in Case B, the effect of hood introduction is negligible. Figure 13, which shows the relationship between hood collection rate and C_{qd} , also shows that in Case B, the decrease in CO₂ concentration (infection risk) with an

increase in hood collection rate is small. This indicates that even after the hood is introduced in Case B, it is not possible to collect the exhaled air of the infected person that reaches the mouth of the non-infected person. Therefore, the hoods were not effective in other areas. Therefore, careful consideration is required when installing local exhaust hoods in areas other than examination rooms.

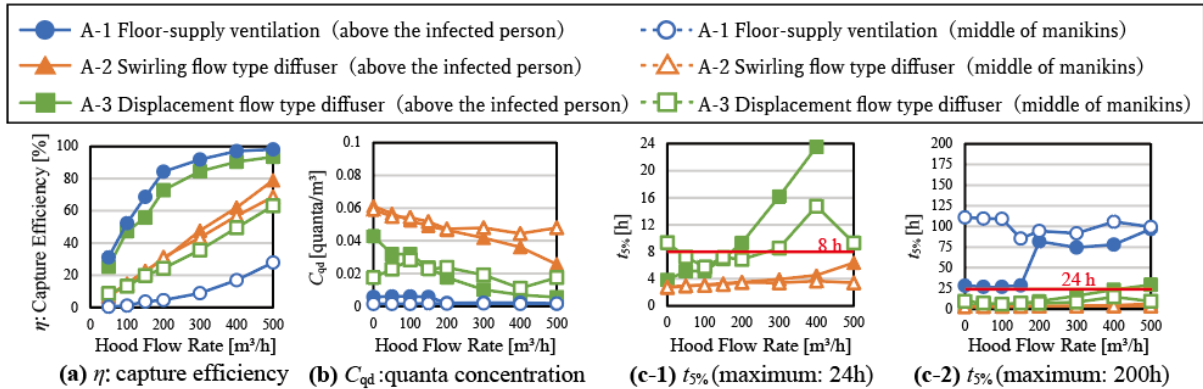


Fig.12 Calculation result of η : capture efficiency, C_{qd} : quanta concentration in front of doctor mouth, $t_{5\%}$: Time until doctor's infection probability reaches 5%, calculated by tracer gas

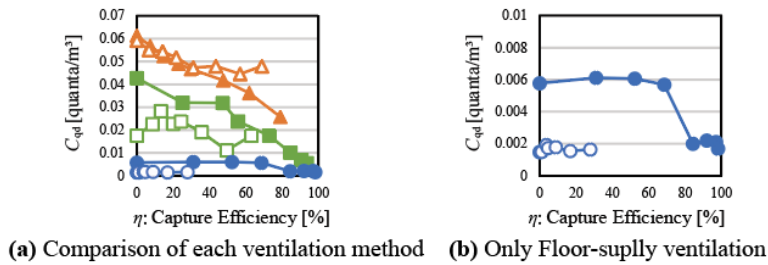


Fig.13 Relationship between η : capture efficiency and C_{qd} : quanta concentration in front of doctor mouth

3.2 The result calculated from artificial saliva

Equation (3) calculates the doctor's infection risk from the simulated saliva particles delivered to the doctor's mouth. The generated amount of simulated saliva particles is estimated by measuring the decrease in simulated saliva before and after the generation (Figure 9). When calculating the density, estimating the particle size and composition of the simulated saliva particles in a state of liquid equilibrium after water evaporation is necessary. Since previous studies (Yang & Marr, 2011) have shown that the final particle size is 0.391 to 0.502 times larger at a relative humidity of 10 to 90%, it was assumed to be 1.0, 0.40, 0.45, and 0.50 times larger. The calculations are based on the assumption that the final particle size is 1.0, 0.40, 0.45, and 0.50 times larger than the final particle size.

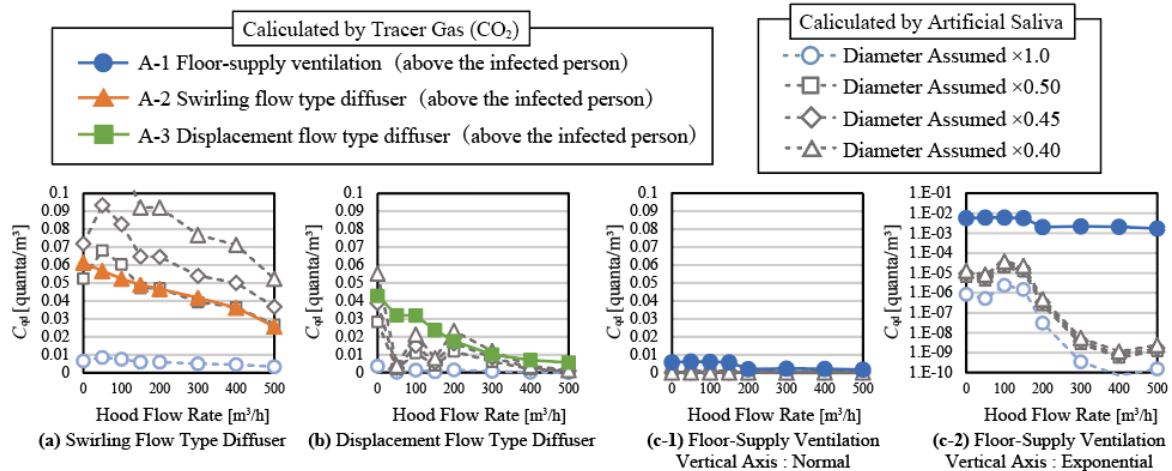


Fig.14 Comparison of C_{qd} (quanta concentration in front of doctor mouth) calculated by tracer gas or artificial saliva particle

Figure 14 shows the results of C_{qd} calculated from quanta concentration before the doctor's mouth and CO₂ when the final particle size was assumed to be 1.0, 0.40, 0.45, and 0.50 times. 0.4 times, the results obtained for the swirling flow type floor blowout (Fig. 14(a)) exceeded those calculated from CO₂. Considering the effects of deposition and adhesion, the results calculated from simulated saliva particles are expected to be smaller than those calculated from CO₂. These results may be because the amount of nebulized saliva was not stable (Figure 8) and the final particle size is not always 0.4 times larger than the final particle size of the simulated saliva particles. When 0.5 times the final particle size was used in the calculation, the C_{qd} was about the same for the swirling flow type blowout (Fig. 14(a)). Therefore, this report calculates C_{qd} and $t_{5\%}$ assuming the final particle diameter is 0.5 times larger.

C_{qd} and $t_{5\%}$ for each condition, calculated assuming that the final particle size is 0.5 times larger than the initial particle size regardless of the initial particle size, are shown in Figure 15. As in the case of the calculation based on the trend CO₂, the risk of infection is lowered in the order of " FSDV > displacement ventilation type floor diffuser > swirling-flow type floor diffuser ". This result reinforces the conclusions from the results calculated from the CO₂.

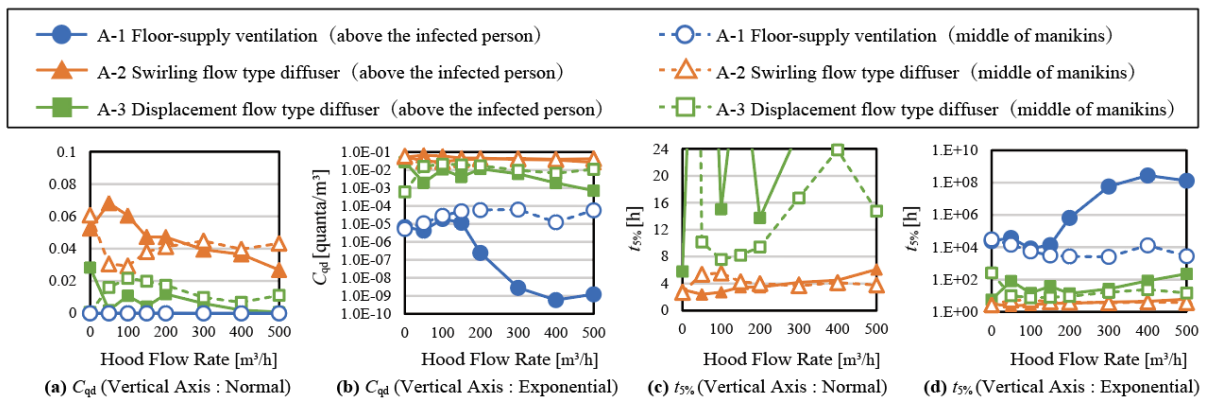


Fig.15 Calculation result of C_{qd} :quanta concentration in front of doctor mouth, $t_{5\%}$:Time until doctor's infection probability reaches 5%, calculated by artificial saliva particle (Assuming Diameter : $D \times 0.5$)

4 CONCLUSION

This study aimed to evaluate the effectiveness of the combination of air conditioning with floor-supply displacement ventilation(FSDV) and a hood and its performance as an infection control measure. The results of the doctor's infection risk calculated from CO₂ and simulated saliva droplets were also discussed. The findings of this study are summarized below.

- The effectiveness of the combination of FSDV and a local exhaust hood was confirmed in the examination rooms, and high infection control performance was confirmed in both the examination rooms and non-examination rooms.
- The high infection control performance confirmed in the non-examination rooms was strongly influenced by the large air supply volume of 1,000 m³/h for the room volume, and careful consideration is required to introduce this system in the non-examination rooms.
- These results were confirmed by both CO₂ gas and simulated saliva particles. These results were confirmed for both CO₂ gas and simulated saliva particles, and the results calculated from the simulated saliva particles were smaller than those calculated from the gas.

Future experiments should be conducted with a more stable nebulizer and closer to the particle

size distribution of the actual conversation.

5 ACKNOWLEDGEMENTS

This study was supported by Grant-in-Aid for Scientific Research (B)21H01492 and Osaka University School of Medicine Research and Development Grant for Novel Coronavirus Countermeasures in 2021.

6 REFERENCES

- Akimoto, T., Nobe, T., Tanabe, S., & Kimura, K. (1997). EXPERIMENTAL STUDY ON INDOOR THERMAL ENVIRONMENT AND VENTILATION PERFORMANCE OF FLOOR-SUPPLY DISPLACEMENT VENTILATION SYSTEM. *Journal of Architecture and Planning (Transactions of AIJ)*, 62(499), 17–25.
https://doi.org/10.3130/AIJA.62.17_3
- Federation of European Heating Ventilation and Air Conditioning Associations. (2020). *COVID-19 guidance document Version 4.0; How to operate HVAC and other building service systems to prevent the spread of the coronavirus (SARS-CoV-2) disease (COVID-19) in workplaces.*
- Komori, M., Yamanaka, T., Kobayashi, T., Choi, N., & Kobayashi, N. (2022). Development of a Design of Local Exhaust Hood with High Capture Efficiency (Part5) Prediction of Airflow under Exhaust Hood by Modeling under Passing Airflow. *Technical Papers of Annual Meeting the Society of Heating, Air-Conditioning and Sanitary Engineers of Japan*, 4, 69–72.
- Morawska, L., Johnson, G., Ristovski, Z., Hargreaves, M., Mengersen, K., Corbett, S., Chao, C., Li, Y., & Katoshevski, D. (2009). Size distribution and sites of origin of droplets expelled during expiratory activities. In *Journal of Aerosol Science* (Issue 3).
<http://eprints.qut.edu.au/>
- Ogata, M., Ichikawa, M., Tsutsumi, H., Ariga, T., Hori, S., & Tanabe, S. I. (2018). Measurement of cough droplet deposition using the cough machine. *Journal of Environmental Engineering (Japan)*, 83(743), 57–64. <https://doi.org/10.3130/aije.83.57>
- Riley EC, Murphy G, & Riley RL. (1978). Airborne spread of measles in a suburban elementary school. *American Journal of Epidemiology*, 107, 421–432.
- Wells, W. F. (1955). *Airborne Contagion and Air Hygiene: An Ecological Study of Droplet Infections - William Firth Wells* -. University of Michigan Libraries.
https://books.google.co.jp/books?hl=ja&lr=lang_ja|lang_en&id=T8nVAAAAMAAJ&oi=fnd&pg=PR7&dq=Wells+WF.+Airborne+Contagion+and+Air+Hygiene.+Cambridge,+MA:+Harvard+University+Press,+1955&ots=dTn_tdoRGZ&sig=7xpun_61NO_NGHTJQQISJZP2fow#v=onepage&q&f=false
- World Health Organization. (2020). Transmission of SARS-CoV-2: implications for infection prevention precautions. *World Health Organization*.
- Yang, W., & Marr, L. C. (2011). Dynamics of Airborne influenza A viruses indoors and dependence on humidity. *PLoS ONE*, 6(6). <https://doi.org/10.1371/journal.pone.0021481>
- Zhang, R., Yamanaka, T., Kobayashi, T., Choi, N., Kobayashi, N., & Yoshihara, J. (2022). *Performance of Local Exhaust System as Prevention Measure of Infection in Consulting Room (Part 3) Exposure Concentration Response and Hood Capture Rate of Droplet Nuclei from Conversation and Coughing Based on Transient CFD Analysis.*